

Circular RNA ANKIB1 alleviates hypoxia-induced cardiomyocyte injury by modulating miR-452-5p/SLC7A11 axis

Gang Li^{1,D}, Xiaolei Tang^{2,C}, Huaping Tang^{1,A,B}

¹ Department of Geriatric Medicine, Maanshan People's Hospital, China

² Department of Clinical Laboratory, The Second Affiliated Hospital of Wannan Medical College, Wuhu, China

A – research concept and design; B – collection and/or assembly of data; C – data analysis and interpretation;

D – writing the article; E – critical revision of the article; F – final approval of the article

Advances in Clinical and Experimental Medicine, ISSN 1899–5276 (print), ISSN 2451–2680 (online)

Adv Clin Exp Med. 2024;33(3):261–272

Address for correspondence

Gang Li

E-mail: gs_yz@163.com

Funding sources

The study was funded by Maanshan Science and Technology Plan Project No. YL-2021-03.

Conflict of interest

None declared

Received on February 14, 2023

Reviewed on April 4, 2023

Accepted on June 12, 2023

Published online on August 7, 2023

Abstract

Background. Acute myocardial infarction (AMI) is a common cardiovascular disease worldwide. Circular RNAs (circRNAs) have been shown to exert essential roles in the progression of AMI. However, it remains unclear whether *circANKIB1* protects cardiomyocytes from hypoxia-induced injury.

Objectives. The aim of the study was to elucidate the function and mechanisms of *circANKIB1* in AMI.

Materials and methods. The expression of RNA was estimated using a quantitative real-time polymerase chain reaction (qPCR) assay, and the level of protein was determined with the use of western blot analysis. Methyl thiazolyl tetrazolium (MTT) assay was introduced to test cell viability, and a terminal deoxynucleotidyl transferase dUTP nick end labeling (TUNEL) assay was used to detect apoptosis. The relative levels of ferrous ion (Fe^{2+}), reactive oxygen species (ROS) and malondialdehyde (MDA) were measured with their corresponding detection kits. The potential target of *circANKIB1* and *miR-452-5p* was predicted using the StarBase database and verified by employing a dual luciferase reporter assay.

Results. This study showed a significant decrease in *circANKIB1* in hypoxia-treated H9c2 cells. Hypoxic exposure significantly reduced the viability of H9c2 cells and the expression of GPX4, and increased the content of Fe^{2+} , ROS and MDA. These effects were reversed by the overexpression of *circANKIB1*. Additionally, *miR-452-5p* was found to be a direct target of *circANKIB1*, and the *miR-452-5p* mimic significantly eliminated the protective effect of *circANKIB1* overexpression in hypoxia-induced cells. In addition, *miR-452-5p* could bind to *SLC7A11* and negatively regulate its expression. The knockdown of *SLC7A11* abolished the effect of *circANKIB1* overexpression on hypoxia-induced cardiomyocyte injury.

Conclusions. This investigation revealed for the first time that *circANKIB1* regulated signaling of the *miR-452-5p/SLC7A11* axis, thereby ameliorating hypoxia-induced cardiomyocyte injury. These findings suggest that *circANKIB1* might be a useful adjunct in the treatment of AMI.

Key words: cardiomyocyte, *SLC7A11*, acute myocardial infarction, *miR-452-5p*, *circANKIB1*

Cite as

Li G, Tang X, Tang H. Circular RNA ANKIB1 alleviates hypoxia-induced cardiomyocyte injury by modulating miR-452-5p/SLC7A11 axis [published online as ahead of print on August 7, 2023]. *Adv Clin Exp Med*. 2024;33(3):261–272. doi:10.17219/acem/168242

DOI

10.17219/acem/168242

Copyright

Copyright by Author(s)

This is an article distributed under the terms of the Creative Commons Attribution 3.0 Unported (CC BY 3.0) (<https://creativecommons.org/licenses/by/3.0/>)

Background

Acute myocardial infarction (AMI), as a cardiovascular disease, is associated with cardiomyocyte injury caused by acute ischemia and hypoxia. Acute myocardial infarction causes severe damage to the myocardium, resulting in high mortality.^{1,2} Previous findings suggest that AMI could induce oxidative stress in cardiomyocytes, ultimately leading to their dysfunction.^{3,4} Exploring the molecular network of cardiomyocyte injury and revealing target genes that protect them from acute ischemia and hypoxia are essential for the treatment of AMI patients.

Circular RNA (circRNA) is highly stable and displays a novel circular structure without 5' or 3' ends.^{5–7} CircRNAs are involved in the regulation of various intracellular activities⁸ and are considered markers in a variety of human diseases. Additionally, scientists have demonstrated that multiple circRNAs play an important role in the progression of AMI.^{9,10} For example, Ren et al. demonstrated that *circ_0023461* knockdown mitigated hypoxia-induced cardiomyocyte injury by mediating the *miR-370-3p/PDE4D* signaling axis.¹¹ Wang et al. discovered that *circUBXN7* improved hypoxia/reoxygenation (H/R)-induced apoptosis and the inflammatory responses in cardiomyocytes by modulating the *miR-622/MCL1* axis signaling.¹² The circRNA ankyrin repeats and IBR domain containing 1 (*circANKIB1*) have been reported to be a splicing product of *ANKIB1* mRNA that regulate the development of multiple cells.^{13,14} Mao et al. revealed that *circANKIB1* was closely related to the process of peripheral nerve injury.¹⁵ However, the role of *circANKIB1* in hypoxia-induced cardiomyocyte injury remains unclear.

MicroRNAs (miRNAs) are another widely studied non-coding RNAs that have been implicated in diverse biological functions, such as cell proliferation.¹⁶ Current investigations have verified that circRNAs could serve as competitive endogenous RNA (ceRNAs) of miRNAs to influence the expression of downstream mRNA.¹⁷ Here, we examined the connection between *circANKIB1* and *miR-452-5p* and explored the effects of *circANKIB1/miR-452-5p* in hypoxia-induced cardiomyocyte injury.

Iron accumulation has been reported to increase the risk of cardiovascular disease (CVD).¹⁸ Ferroptosis is a recently discovered mode of cell death characterized by iron-dependent lipid peroxides increased into the toxic range.^{19,20} In addition, Fang et al. reported that ferroptosis can modulate ischemia–reperfusion-induced cardiomyopathy.¹⁹ Therefore, revealing the regulators of ferroptosis is crucial for finding the appropriate therapeutic measures for AMI. The *SLC7A11* is a multichannel transmembrane protein that prevents the development of ferroptosis by increasing glutathione (GSH) synthesis and reducing the accumulation of lipid oxide.^{21,22} Our previous study found that *SLC7A11* is an important potential target for *miR-452-5p*. However, whether *circANKIB1/miR-452-5p* mediates ferroptosis of cardiomyocytes under hypoxia conditions by *SLC7A11* is yet to be explored.

Objectives

We hypothesized that *circANKIB1* plays a key role in hypoxia-induced cardiomyocyte injury by regulating *SLC7A11*-associated ferroptosis, which would provide a promising therapeutic network for the treatment of AMI.

Materials and methods

Cell culture

Rat H9c2 cardiomyocytes (BNCC337726) were obtained from the BeNa Culture Collection (Beijing, China) and maintained in Dulbecco's modified Eagle's medium (DMEM; SH30022.LS; Hyclone, Logan, USA) with 10% fetal bovine serum (FBS; F8318; Sigma-Aldrich, St. Louis, USA) and 1× Penicillin-Streptomycin (P1400; Solarbio, Beijing, China) at 37°C and 5% CO₂.²³

Hypoxia model

The hypoxia model was completed as described in the previous report.¹¹ The H9c2 cells were subjected to hypoxic conditions (O₂:CO₂:N₂ = 1:5:94) for 24 h, 48 h and 72 h, and then cultured under normoxia conditions (O₂:CO₂:N₂ = 21:5:74) for an additional 6 h to simulate AMI in vitro. The H9c2 cells cultured for 30 h under normoxia conditions (O₂:CO₂:N₂ = 21:5:74) were considered control cells.

Cell transfection

The vector with *circANKIB1* (oe-*circANKIB1*) and the empty vector (vector) were obtained from Hunan Fenghui Biotechnology Co. Ltd. (Hunan, China). Small interfering RNA (siRNA) targeting the *SLC7A11* sequence (si-*SLC7A11*) and the corresponding scrambled control (si-NC) were synthesized by Sangon Biotech (Shanghai, China). The *miR-452-5p* mimic/inhibitor and its control (mimic/inhibitor)-NC were obtained from Guangzhou Ruibo Biotechnology Co. Ltd. (Guangzhou, China). Lipofectamine™ 2000 Transfection Reagent (L7800; Solarbio) was used to transfect all vectors (4 µg) and oligonucleotides (50 nM) into H9c2 cells.²⁴

qPCR assay

Total RNA was extracted from H9c2 cells using Trizol™ reagent (Invitrogen, Waltham, USA). NanoDrop™ 2000 nucleic acid analyzer (Thermo Fisher Scientific, Waltham, USA) was used to detect the concentration and purity of RNA to confirm that the A260/A280 ratio was 1.9–2.1, according to the Minimum Information for Publication of Quantitative Real-Time PCR Experiments

Table 1. Quantitative real-time polymerase chain reaction (qPCR) primers

Genes	Primers (forward)	Primers (reverse)
<i>circANKIB1</i>	5'-AGACCGCAGACATGCTCC-3'	5'-AGTCCCTAATATCTTATTCATCCA-3'
<i>miR-452-5p</i>	5'-GCGCAACTGTTGCAGAG-3'	5'-GTGCAGGGTCCGAGGT-3'
<i>SLC7A11</i>	5'-GCTGACACTCGTGCTATT-3'	5'-ATTCTGGAGGTCTTTGGT-3'
<i>U6</i>	5'-CTCGCTTCGGCAGCACA-3'	5'-AACGCTTCACGAATTTGCGT-3'
<i>GAPDH</i>	5'-GGGAGCCAAAGGGTCAT-3'	5'-GAGTCCTCCACGATACCAA-3'

(MIQE) guidelines.²⁵ The RNA was reverse-transcribed into complementary DNA (cDNA) utilizing the Evo M-MLV RT Master Mix (AG11706; Accurate Biology, Hunan, China). Then, a quantitative polymerase chain reaction (qPCR) analysis was performed using the qPCR kit (RK02001; BioMarker Technologies, Beijing, China) on the QuantStudio 5 RT fluorescence qPCR instrument system (BJ005277; ABI, Hunan, China). The following parameters were used for qPCR: 1 cycle at 98°C for 3 min, followed by 40 cycles for 15 s at 94°C, 30 s at 60°C and 1 min at 72°C. The U6 served as the internal reference for *miR-452-5p*, while glyceraldehyde-3-phosphate dehydrogenase (GAPDH) was the internal reference for *circANKIB1*. The $2^{-\Delta\Delta C_t}$ method was utilized to estimate the levels of *miR-452-5p* and *circANKIB1*.²³ All primers (synthesized by BGI Group, Shenzhen, China) are shown in Table 1.

RNase R assay

The extracted RNA was treated with 1 U/ μ g RNase R (14606ES72; YESEN, Shanghai, China) for 30 min, followed by quantitative real-time polymerase chain reaction (qPCR) analysis to detect the expression of *circANKIB1* and liner ANKIB1. A sample of non-processed RNA was considered the control group.²⁶

Subcellular localization assay

A PARIS kit (AM1921; Invitrogen) was used to isolate cytoplasmic and nuclear RNA from H9c2 cells. The qPCR was then performed to determine the content of *circANKIB1* distributed in the cytoplasm or nucleus in H9c2 cells. The *GAPDH* and *U6* served as the housekeeping genes for the cytoplasm and nucleus, respectively.²⁷

Methyl thiazolyl tetrazolium (MTT) assay

Cell viability was tested by employing the MTT Cell Proliferation Assay Kit (40206ES76; YESEN). Briefly, the transfected H9c2 cells were cultured overnight in 96-well plates (3×10^3 cells/well), and cell transfection was performed for 48 h. Then 10 μ L of MTT was added to each well for 4 h. The optical density (OD) was recorded at 570 nm with a microplate reader (SpectraMax Mini; Molecular Devices Ltd., Shanghai, China).²⁸

Reactive oxygen species and malondialdehyde detection

For the detection of reactive oxygen species (ROS), cells were incubated with a 2'-7'-dichlorofluorescein diacetate (DCFH-DA) probe (10 μ M; Beyotime Biotechnology, Shanghai, China) for 30 min in darkness at room temperature. Then, the cells were rinsed twice with phosphate-buffered saline (PBS) and imaged with a fluorescent microscope (Leica DM1000; Leica Camera, Wetzlar, Germany). The fluorescence intensity was examined using a fluorescent microplate reader (Epoch2; BioTek, Vermont, USA; excitation/emission 488/525 nm). The level of ROS and malondialdehyde (MDA) in H9c2 cells was estimated using the ROS assay kit (CA1410; Solarbio) or the MDA assay kit (BC0025; Solarbio), respectively.²⁹

Iron detection

The ferrous ion (Fe^{2+}) in H9c2 cells was monitored using a Fe^{2+} assay kit (BC5415; Solarbio), following the manufacturer's protocol. Briefly, supernatants of conditioned media from cells were placed onto 96-well plates and then incubated with a 5-microliter iron reducer at 25°C for 30 min to detect total iron content. Then, in a dark environment, samples were incubated with 100 μ L of the iron probe for 60 min at 25°C. Finally, the OD was measured at 594 nm with a microplate reader (SpectraMax Mini; Molecular Devices Ltd.).²⁹

Luciferase activity

The *circANKIB1* or *SLC7A11* fragments containing wild-type (WT) or mutant-type (MUT) binding sites with *miR-452-5p* were cloned into pmirGLO vectors (VT1439; YouBio, China). Four luciferase vectors (*circANKIB1*-WT, *circANKIB1*-MUT, *SLC7A11*-WT, and *SLC7A11*-MUT) were then obtained. The H9c2 cells (4×10^5 cells/well) were transfected with *miR-452-5p* mimic/NC (25 nM final concentration) and *circANKIB1*-WT/*circANKIB1*-MUT (2 μ g) or *SLC7A11*-WT/*SLC7A11*-MUT (2 μ g) using Lipofectamine™ 2000 Transfection Reagent (L7800; Solarbio). Then, the luciferase activity of Renilla (normalized as the control) and Firefly was tested with a Dual-Lucy Assay Kit (D0010; Solarbio) on a microplate reader (SpectraMax Mini; Molecular Devices Ltd.).²³

Western blotting analysis

The total protein of H9c2 cells was collected using radioimmunoprecipitation assay (RIPA) lysis buffer (R0020; Solarbio) and isolated on a sodium dodecyl sulfate-polyacrylamide gel electrophoresis (SDS-PAGE), and then transferred to polyvinylidene fluoride (PVDF) membranes (YA1701; Solarbio). The membranes were treated using Tris-buffered saline (TBS) containing 3% skim milk (T476445-10EA; Aladdin, Shanghai, China) at 4°C for 1 h and then incubated with the primary antibodies, including anti-GPX4 (1:1000, 14432-1-AP; Proteintech, Rosemont, USA), anti-SLC7A11 (1:1000, 26864-1-AP; Proteintech) and anti- β -actin (1:1000, ab8227; Abcam, Cambridge, UK). Finally, the membrane was treated with the secondary antibody (1:2000, goat anti-rabbit

IgG antibody, bs-0295G; Bioss, Beijing, China) for 2 h and enhanced chemiluminescence (ECL) detection solutions (HR0340, E266188; Aladdin) to observe the protein bands.²⁴

TUNEL assay

Cells were fixed in 4% paraformaldehyde for 30 min, followed by incubation with 0.3% Triton X-100 for 5 min. Then, the cells were incubated using terminal deoxynucleotidyl transferase dUTP nick end labeling (TUNEL) detection buffer (Beyotime Biotechnology) for 1 h. The 4',6-diamidino-2-phenylindole (DAPI) was applied to counterstain the nuclei. The cells were observed under a fluorescence microscope (Leica DM1000; Leica Camera), and the TUNEL-positive cells were counted.³⁰

Table 2. The results of t-test and ANOVA

Figure	Method	F (DFn, DFd)	t	df	p _{sk}	p _L
Figure 1A	ANOVA	F (3,8) = 230.4	–	–	>0.1	0.6704
Figure 1B	ANOVA	F (3,8) = 123.3	–	–	>0.1	0.9921
Figure 1C	ANOVA	F (1,8) = 494.8	–	–	>0.1	0.8131
Figure 1D	ANOVA	F (2,12) = 939.9	–	–	>0.1	0.7471
Figure 2A	Student's t-test	–	57.88	4	>0.1	0.9988
Figure 2B	ANOVA	F (3,8) = 148.2	–	–	>0.1	0.9846
Figure 2C	ANOVA	F (3,8) = 230.3	–	–	>0.1	0.9163
Figure 2D	ANOVA	F (3,8) = 358.5	–	–	>0.1	0.9535
Figure 2E	ANOVA	F (3,8) = 342.0	–	–	>0.1	0.9003
Figure 2F	ANOVA	F (3,8) = 131.7	–	–	>0.1	0.9024
Figure 3B	Student's t-test	–	35.18	4	>0.1	0.9968
Figure 3C	ANOVA	F (1,8) = 168.1	–	–	>0.1	0.6943
Figure 3D	ANOVA	F (3,8) = 294.2	–	–	>0.1	0.7502
Figure 3E	ANOVA	F (3,8) = 164.1	–	–	>0.1	0.9279
Figure 4A	ANOVA	F (3,8) = 202.4	–	–	>0.1	0.7200
Figure 4B	ANOVA	F (3,8) = 427.5	–	–	>0.1	0.9888
Figure 4C	ANOVA	F (3,8) = 291.3	–	–	>0.1	0.9603
Figure 4D	ANOVA	F (3,8) = 240.9	–	–	>0.1	0.8582
Figure 4E	ANOVA	F (3,8) = 147.3	–	–	>0.1	0.9645
Figure 5B	ANOVA	F (1,8) = 197.4	–	–	>0.1	0.6893
Figure 5C	ANOVA	F (3,8) = 60.41	–	–	>0.1	0.9097
Figure 5D	ANOVA	F (3,8) = 57.63	–	–	>0.1	0.9688
Figure 5E	ANOVA	F (3,8) = 164.7	–	–	>0.1	0.9932
Figure 5F	ANOVA	F (3,8) = 215.5	–	–	>0.1	0.8702
Figure 6A	Student's t-test	–	13.63	4	>0.1	0.8026
Figure 6B	ANOVA	F (3,8) = 234.7	–	–	>0.1	0.8439
Figure 6D	ANOVA	F (3,8) = 182.8	–	–	>0.1	0.8641
Figure 7B	ANOVA	F (3,8) = 242.3	–	–	>0.1	0.6751
Figure 7C	ANOVA	F (3,8) = 87.08	–	–	>0.1	0.4217
Figure 7D	ANOVA	F (3,8) = 126.6	–	–	>0.1	0.3352
Figure 7E	ANOVA	F (3,8) = 91.43	–	–	>0.1	0.9008

ANOVA – analysis of variance; df – degrees of freedom; t – Student's t-test results; p_{sk} – Shapiro–Wilk test; p_L – Levene's test; DFd – degrees of freedom denominator; DFn – degrees of freedom numerator.

Statistical analyses

The analysis was conducted using GraphPad Prism v. 8.0 software (GraphPad Software, San Diego, USA), and all data were presented as mean \pm standard deviation ($M \pm SD$). Student's t-test or one-way analysis of variance (ANOVA) followed by Tukey's post hoc test were used to analyze differences between 2 groups or multiple groups, respectively. The normality of the data and the homogeneity of variance between groups were tested using the Shapiro–Wilk test and Levene's test, respectively. The value of $p > 0.05$ indicated that the assumption of normality of data and homogeneity of variance were consistent, and further parameter testing could be performed. Statistical significance was set at $p < 0.05$.¹³ The results of the statistical analyses are presented in Table 2 and Table 3.

Results

Overexpression of *circANKIB1* ameliorates hypoxia-induced cardiomyocyte injury and ferroptosis

The expression levels of HIF1 α , which is an indicator of hypoxia,³¹ were detected in H9c2 cells following hypoxia treatment. The expression of HIF1 α was significantly increased in H9c2 cells after hypoxia treatment for 24 h, 48 h and 72 h compared with normoxic H9c2 cells (Fig. 1A). The results indicated that the hypoxia-induced cardiomyocyte model was successfully established. As hypoxia treatment over a long duration may result in irreversible damage to H9c2 cells, 24 h timepoint was selected for subsequent experiments (Fig. 1A). We demonstrated that *circANKIB1* expression was significantly decreased in a time-dependent manner under hypoxic conditions

Table 3. Tukey's post hoc test results of ANOVA

Figure	Method	p_s	p_{T1}	p_{T2}	p_{T3}
Figure 1A	ANOVA	0.0001	0.0002	0.0001	0.0001
Figure 1B	ANOVA	0.0001	0.0045	0.0001	0.0001
Figure 1C	ANOVA	0.0001	0.0665	0.0001	–
Figure 1D	ANOVA	0.0001	0.0001	0.0001	0.0001
Figure 2B	ANOVA	0.0001	0.0001	0.0001	–
Figure 2C	ANOVA	0.0001	0.0001	0.0001	–
Figure 2D	ANOVA	0.0001	0.0001	0.0001	–
Figure 2E	ANOVA	0.0001	0.0001	0.0001	–
Figure 2F	ANOVA	0.0001	0.0001	0.0001	–
Figure 3C	ANOVA	0.0001	0.9425	0.0001	–
Figure 3D	ANOVA	0.0001	0.0011	0.0001	0.0001
Figure 3E	ANOVA	0.0001	0.0001	0.0001	–
Figure 4A	ANOVA	0.0001	0.0001	0.0001	0.0001
Figure 4B	ANOVA	0.0001	0.0001	0.0001	0.0001
Figure 4C	ANOVA	0.0001	0.0001	0.0001	0.0001
Figure 4D	ANOVA	0.0001	0.0001	0.0001	0.0001
Figure 4E	ANOVA	0.0001	0.0001	0.0001	0.0001
Figure 5B	ANOVA	0.0001	0.0001	0.7740	–
Figure 5C	ANOVA	0.0001	0.0193	0.0002	0.0001
Figure 5D	ANOVA	0.0001	0.0001	0.0001	–
Figure 5E	ANOVA	0.0001	0.0001	0.0001	–
Figure 5F	ANOVA	0.0001	0.0001	0.0001	–
Figure 6B	ANOVA	0.0001	0.0001	0.0001	0.0001
Figure 6D	ANOVA	0.0001	0.0001	0.0001	0.0001
Figure 7B	ANOVA	0.0001	0.0001	0.0001	0.0001
Figure 7C	ANOVA	0.0001	0.0001	0.0001	0.0002
Figure 7D	ANOVA	0.0001	0.0001	0.0001	0.0001
Figure 7E	ANOVA	0.0001	0.0001	0.0001	0.0001

ANOVA – analysis of variance; p_s – p-value summary of ANOVA; p_T – Tukey's post hoc test results. The p-values of the comparison results between the different groups were divided into $p_{T1/2/3}$, respectively.

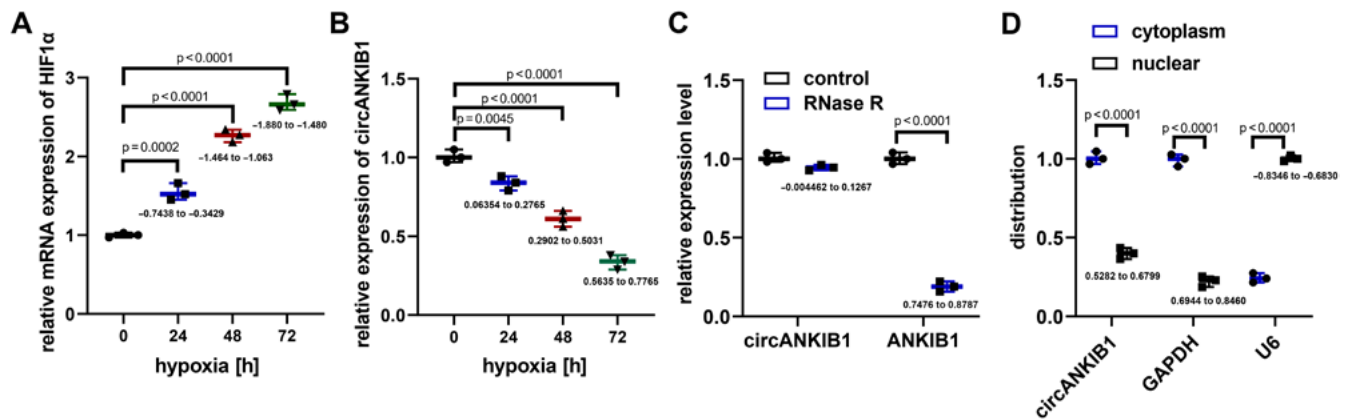


Fig. 1. The overexpression of *circANKIB1* ameliorates hypoxia-induced cardiomyocyte injury and ferroptosis. **A.** Hypoxia-inducible factor (HIF)1α mRNA expression level in H9c2 cells was increased after hypoxia treatment for 24 h, 48 h or 72 h tested with quantitative real-time polymerase chain reaction (qPCR) assay ($p = 0.001$, $n = 3$, analysis of variance (ANOVA) test); **B.** *CircANKIB1* expression level was decreased in H9c2 cells after hypoxia treatment for 0 h, 24 h, 48 h, or 72 h ($p = 0.001$, $n = 3$, ANOVA test); **C.** RNase R assay and qPCR assay were used to test the expression level of *circANKIB1* or liner and it was found that there was no significant change in *circANKIB1* expression, while liner ANKIB1 expression was decreased ($p = 0.001$, $n = 3$, ANOVA test); **D.** The distribution of *circANKIB1* was confirmed using subcellular localization assay ($p = 0.001$, $n = 3$, ANOVA test)

compared to normoxic H9c2 cells (Fig. 1B). To reveal the properties of *circANKIB1*, we carried out an RNase R assay and discovered that *circANKIB1* effectively blocked the degradation of RNase R, implying that *circANKIB1* was more stable than liner ANKIB1 (Fig. 1C). Furthermore, subcellular localization assays demonstrated that *circANKIB1* was localized in the cytoplasm of H9c2 cardiomyocytes more than in the nucleus (Fig. 1D). These data indicated that *circANKIB1* was a stable circRNA that might be involved in the progression of hypoxia-induced cardiomyocyte injury.

Overexpression of *circANKIB1* inhibited hypoxia-induced cardiomyocyte injury and ferroptosis

To investigate the effect of *circANKIB1* on hypoxia-triggered cardiomyocyte injury, we performed overexpression experiments in H9c2 cells (Fig. 2A). Cell viability was estimated using the MTT assay, which showed that hypoxia suppressed the viability of H9c2 cells, which was notably restored by *circANKIB1* overexpression (Fig. 2B). Interestingly, the level of iron was significantly reduced in H9c2 cells with *circANKIB1* overexpression compared with control cells, which implied that *circANKIB1* was likely to be associated with the progression of ferroptosis (Fig. 2C). Notably, the accumulation of ROS and lipid peroxidation (MDA) is considered an important factor in ferroptosis.³² Therefore, the levels of ROS and MDA in H9c2 cells after the overexpression of *circANKIB1* were detected. The data demonstrated that hypoxia dramatically increased the accumulation of ROS and MDA, which was effectively reversed by the overexpression of *circANKIB1* (Fig. 2D,E). The GPX4, an inhibitor of ferroptosis,³³ was also investigated. After H/R treatment, GPX4 was decreased in H9c2 cells, whereas overexpressed *circANKIB1* significantly upregulated GPX4 (Fig. 2F). Taken together,

these data suggest that the overexpression of *circANKIB1* inhibited ferroptosis from alleviating hypoxia-induced cardiomyocyte injury.

miR-452-5p negatively interacts with *circANKIB1* in hypoxic H9c2 cells

We used the starBase database (<http://starbase.sysu.edu.cn/>) to predict the target miRNA of *circANKIB1*. We found that *miR-452-5p* contains binding sequences of *circANKIB1* (Fig. 3A). The *miR-452-5p* mimics were obtained to upregulate *miR-452-5p* expression in H9c2 cells, and functional analyses were performed (Fig. 3B). The luciferase assay showed that *miR-452-5p* mimics decreased the luciferase activity of circANKIB1-WT but not circANKIB1-MUT (Fig. 3C). Additionally, the expression level of *miR-452-5p* was significantly upregulated in hypoxia-treated cells, compared with normoxic H9c2 cells (Fig. 3D). Furthermore, to observe the regulatory influence of *circANKIB1* on *miR-452-5p* expression, H9c2 cells were transfected with oe-*circANKIB1* or a vector, followed by the examination of *miR-452-5p* expression using qPCR. The results demonstrated a decrease in *miR-452-5p* expression after the overexpression of *circANKIB1* in H9c2 cells under both normoxic and hypoxic conditions (Fig. 3E).

miR-452-5p mimic reversed the regulation of *circANKIB1* on hypoxia-induced cardiomyocyte injury and ferroptosis

To verify whether *miR-452-5p* was associated with the protective effect of *circANKIB1* in cardiomyocyte injury, we transfected a *miR-452-5p* mimic into H9c2 cells with *circANKIB1* overexpression and performed a series of functional experiments. The MTT assay indicated that the *miR-452-5p* mimic effectively counteracted *circANKIB1* overexpression regarding the viability

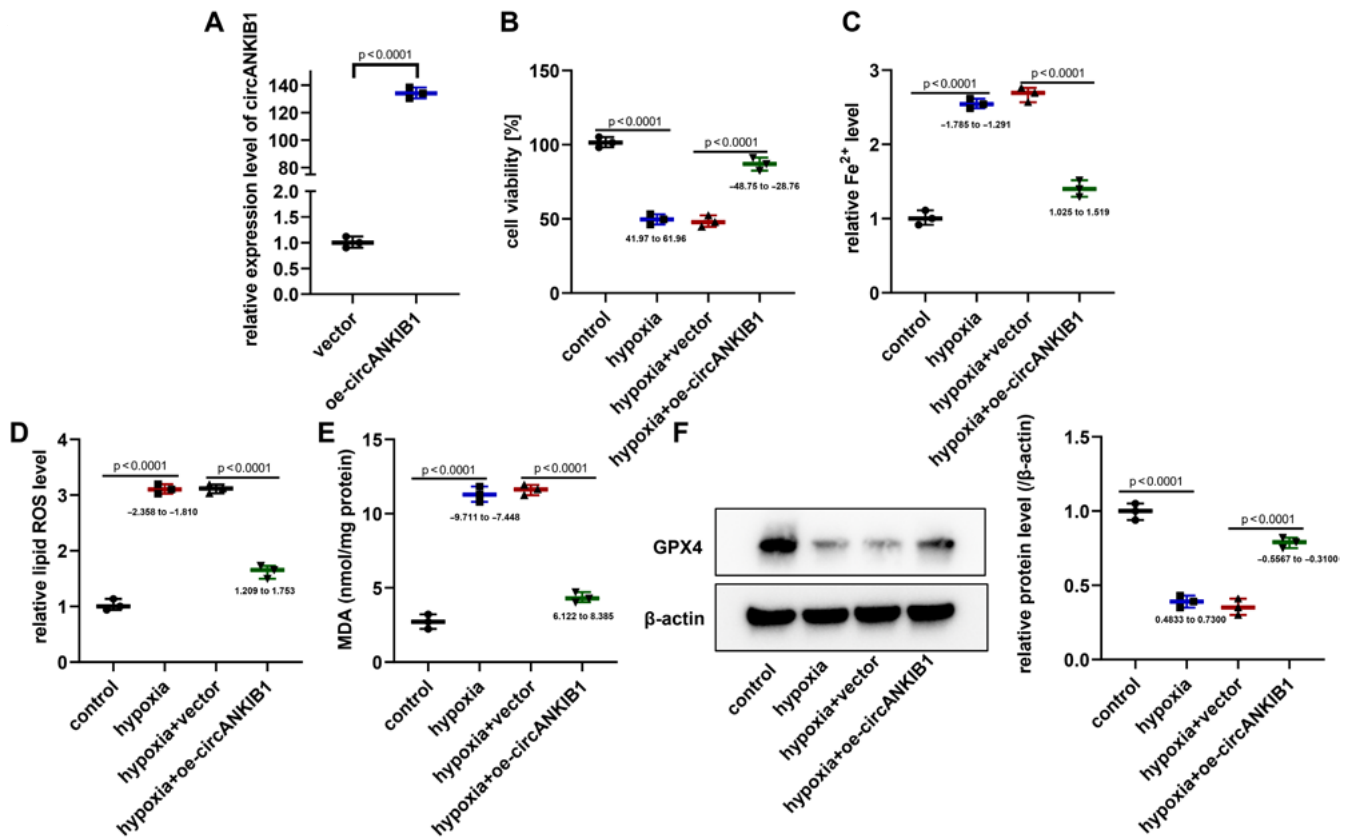


Fig. 2. The overexpression of *circANKIB1* improved hypoxia-induced cardiomyocyte injury and ferroptosis. **A.** The expression level of *circANKIB1* was increased and tested with quantitative real-time polymerase chain reaction (qPCR) assay ($p = 0.001$, $n = 3$, Student's *t*-test); **B.** Methyl thiazolyl tetrazolium (MTT) assay monitored that cell viability was suppressed by hypoxia and could be restored by *circANKIB1* overexpression ($p = 0.001$, $n = 3$, analysis of variance (ANOVA) test); **C–E.** The reduced expression of ferrous ion (Fe^{2+}) (**C**), reactive oxygen species (ROS) (**D**) and malondialdehyde (MDA) (**E**) was analyzed using corresponding kits ($p = 0.001$, $n = 3$, ANOVA test); **F.** The increased GPX4 expression was examined with western blotting analysis ($n = 3$, ANOVA test)

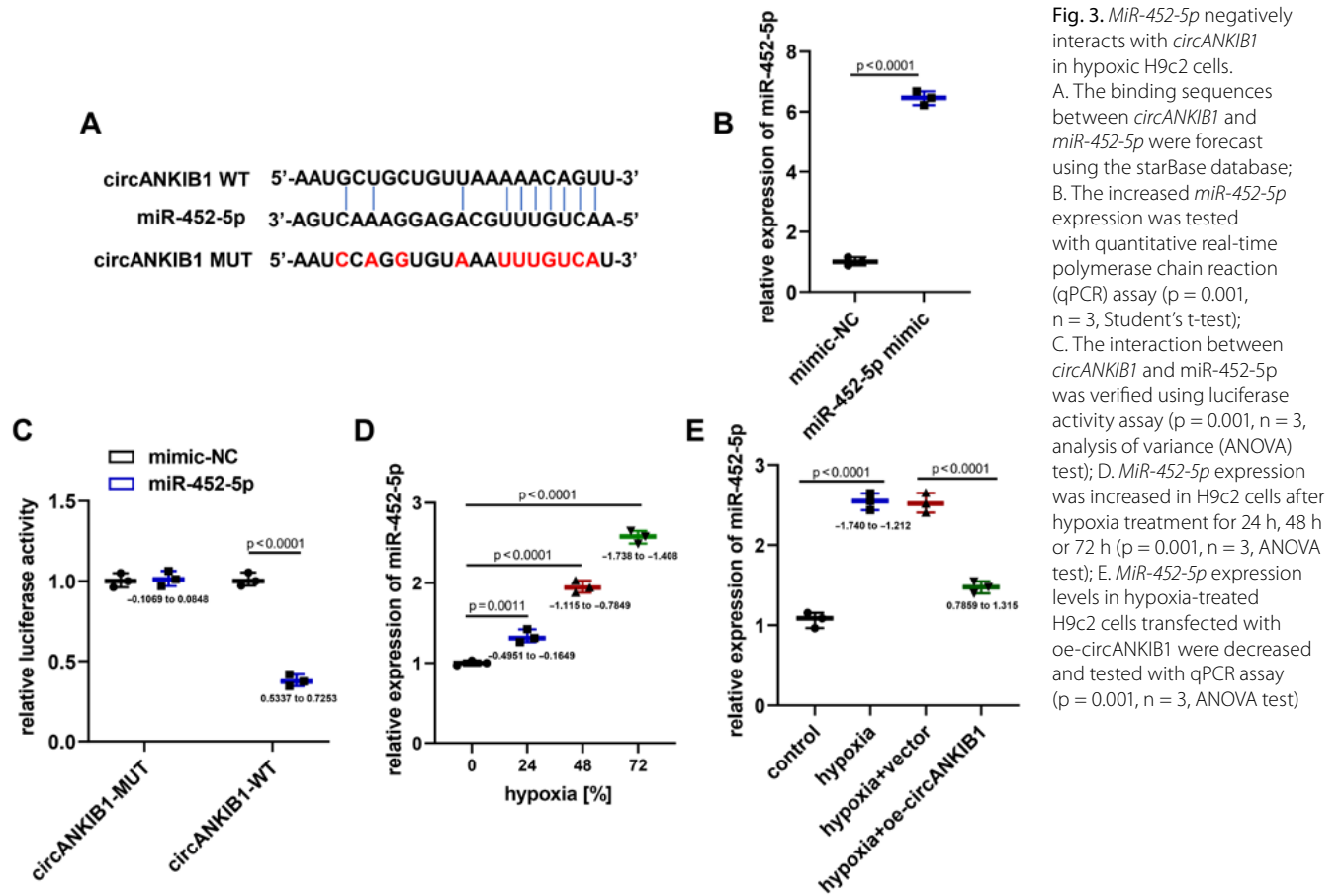


Fig. 3. *MiR-452-5p* negatively interacts with *circANKIB1* in hypoxic H9c2 cells. **A.** The binding sequences between *circANKIB1* and *miR-452-5p* were forecast using the starBase database; **B.** The increased *miR-452-5p* expression was tested with quantitative real-time polymerase chain reaction (qPCR) assay ($p = 0.001$, $n = 3$, Student's *t*-test); **C.** The interaction between *circANKIB1* and *miR-452-5p* was verified using luciferase activity assay ($p = 0.001$, $n = 3$, analysis of variance (ANOVA) test); **D.** *MiR-452-5p* expression was increased in H9c2 cells after hypoxia treatment for 24 h, 48 h or 72 h ($p = 0.001$, $n = 3$, ANOVA test); **E.** *MiR-452-5p* expression levels in hypoxia-treated H9c2 cells transfected with oe-*circANKIB1* were decreased and tested with qPCR assay ($p = 0.001$, $n = 3$, ANOVA test)

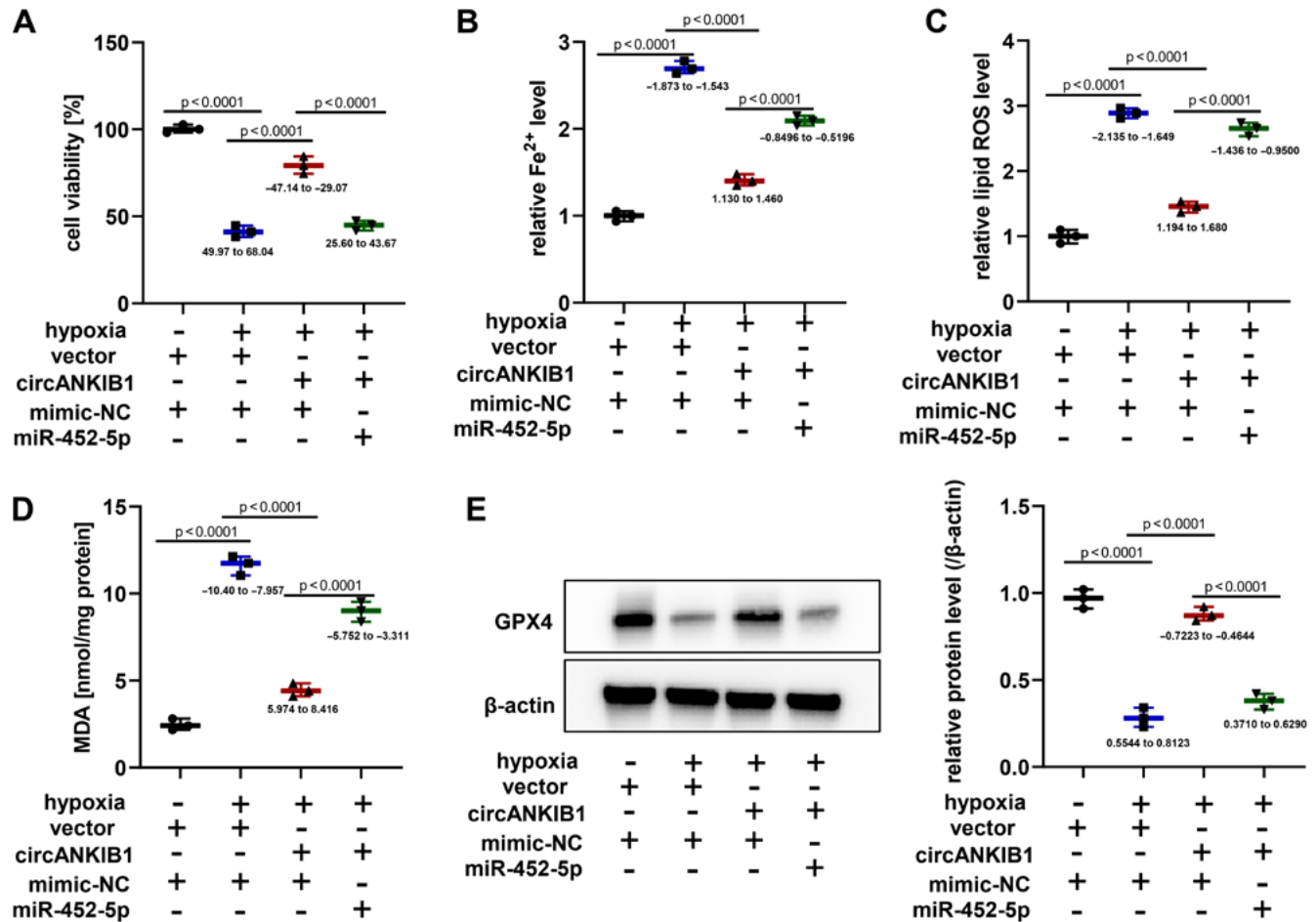


Fig. 4. MiR-452-5p mimic reversed the regulation of *circANKIB1* on hypoxia-induced cardiomyocyte injury and ferroptosis. **A.** Methyl thiazolyl tetrazolium (MTT) assay confirmed that cell viability induced in H9c2 cells by co-transfection with *circANKIB1* overexpression was effectively counteracted by miR-452-5p mimic ($p = 0.001$, $n = 3$, analysis of variance (ANOVA) test); **B–D.** Corresponding kits showed that the reduced levels of ferrous ion (Fe^{2+}) (**B**), reactive oxygen species (ROS) (**C**) and malondialdehyde (MDA) (**D**) were effectively counteracted by miR-452-5p mimic ($p = 0.001$, $n = 3$, ANOVA test); **E.** Western blotting analysis showed that GPX4 expression elevated by the overexpression of *circANKIB1* was eliminated by the miR-452-5p mimic ($p = 0.001$, $n = 3$, ANOVA test)

of hypoxia-treated H9c2 cells (Fig. 4A). Furthermore, the inhibitory effect of overexpressed *circANKIB1* on iron, ROS and MDA accumulation was notably reversed by miR-452-5p mimics in hypoxia-induced H9c2 cells (Fig. 4B–D). Moreover, the overexpression of *circANKIB1* elevated the expression of GPX4 in hypoxia-induced H9c2 cells, and this effect was significantly reduced by the miR-452-5p mimic (Fig. 4E). These data imply that *circANKIB1* exerts its protective role in cardiomyocytes by mediating the expression of *miR-452-5p*.

SLC7A11 is a candidate target of *miR-452-5p* in hypoxia-treated H9c2 cells

A further analysis predicted that *miR-452-5p* would be able to bind to the 3'UTR of *SLC7A11* (Fig. 5A). Results collected from a dual-luciferase reporter gene assay suggested that the miR-452-5p mimic decreased luciferase activity in *SLC7A11*-WT, while the activity of *SLC7A11*-MUT was not affected (Fig. 5B). Furthermore, the expression level of *SLC7A11* was significantly decreased by hypoxia

treatment in a time-dependent manner compared with normoxic H9c2 cells (Fig. 5C). The qPCR and western blotting analyses showed that hypoxia reduced *SLC7A11* mRNA and protein expression, which was effectively restored by a miR-452-5p inhibitor (Fig. 5D,E). Moreover, to observe the regulatory influence of *circANKIB1* on *SLC7A11* expression, H9c2 cells were transfected with oe-*circANKIB1* or vector, followed by an examination of *SLC7A11* expression using western blot. The results highlighted that after the overexpression of *circANKIB1* in H9c2 cells, the expression of *SLC7A11* was elevated, and this could be effectively restored by the miR-452-5p inhibitor (Fig. 5F).

Silencing *SLC7A11* reversed the decreased cell apoptosis effect of *circANKIB1* overexpression on hypoxia-induced cardiomyocyte injury

To confirm the role of *SLC7A11* in hypoxia-treated cardiomyocyte injury, we constructed a vector with a *SLC7A11* knockdown for rescue experiments (Fig. 6A). Cell viability

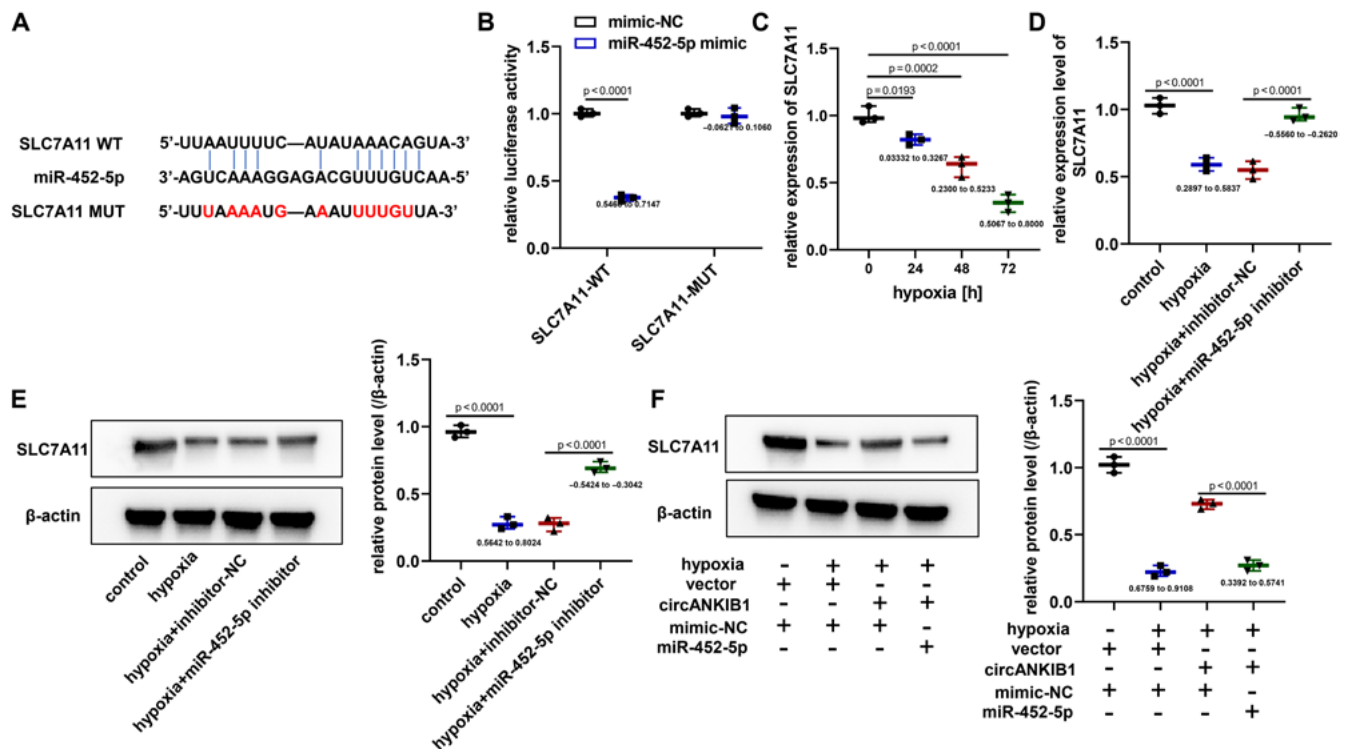


Fig. 5. *SLC7A11* is a candidate target of *miR-452-5p* in hypoxia-treated H9c2 cells. **A.** The binding sites between *miR-452-5p* and *SLC7A11* were forecast via the starBase database; **B.** The interaction between *miR-452-5p* and *SLC7A11* was verified using luciferase activity assay ($p = 0.001$, $n = 3$, analysis of variance (ANOVA) test); **C.** Decreased *SLC7A11* expression level in H9c2 cells after hypoxia treatment for 24 h, 48 h or 72 h was tested with quantitative real-time polymerase chain reaction (qPCR) assay ($p = 0.001$, $n = 3$, ANOVA test); **D,E.** Western blotting analysis and qPCR showed that hypoxia reduced *SLC7A11* mRNA and protein expression, which was effectively restored by *miR-452-5p* inhibitor ($p = 0.001$, $n = 3$, ANOVA test); **F.** The increased protein level of *SLC7A11* expression in hypoxia-treated H9c2 cells transfected with *circANKIB1* overexpression was effectively restored by the *miR-452-5p* inhibitor and tested using western blotting analysis ($p = 0.001$, $n = 3$, ANOVA test)

restoration through *circANKIB1* overexpression was significantly reduced by *SLC7A11* silencing in hypoxic-treated H9c2 cardiomyocytes (Fig. 6B). Then, we explored the effect of *SLC7A11* downregulation in H9c2 cells with various treatments using si-*SLC7A11*. The number of TUNEL-positive cells with transfected with si-*SLC7A11* was markedly increased when compared with *circANKIB1* overexpression transfection in hypoxia-induced H9c2 cells (Fig. 6C,D).

Downregulation of *SLC7A11* reversed the decreased ferroptosis effect of *circANKIB1* overexpression on hypoxia-induced H9c2 cardiomyocytes

The suppressive roles of overexpressed *circANKIB1* on the accumulation of iron, ROS and MDA were effectively counteracted by *SLC7A11* knockdown (Fig. 7A–C). In addition, the decreased Fe^{2+} level in *circANKIB1* overexpression in H9c2 cells was markedly elevated after the transfection with si-*SLC7A11* (Fig. 7D). Furthermore, the overexpression of *circANKIB1* increased GPX4 expression in H9c2 cells under hypoxic conditions, which was notably reversed by *SLC7A11* knockdown (Fig. 7E). Collectively, our findings demonstrated that *circANKIB1* protected cardiomyocytes from hypoxia-induced injury by mediating the *miR-452-5p/SLC7A11* axis.

Discussion

Our research revealed that *circANKIB1* was a stable circRNA that was mainly distributed in the cytoplasm and decreased in hypoxia-treated H9c2 cells. The overexpression of *circANKIB1* significantly inhibited the progression of ferroptosis and protected H9c2 cardiomyocytes from hypoxia-induced injury. In addition, *miR-452-5p* is considered a direct target of *circANKIB1*, and a *miR-452-5p* mimic notably reversed the effect of *circANKIB1* overexpression on ferroptosis and injury in cardiomyocytes induced by hypoxia. Moreover, *SLC7A11* was a potential target for *miR-452-5p*, and *SLC7A11* silencing abolished the protective role of *circANKIB1* against hypoxia-induced cardiomyocyte injury.

Increasing evidence has shown that circRNAs exert vital roles in human CVDs.^{9,34,35} For example, *circRbms1* is highly expressed in AMI, and the loss of *circRbms1* effectively blocked H_2O_2 -related cardiomyocyte apoptosis and ROS accumulation by mediating the *miR-92a/BCL2L1* axis.³⁶ Therefore, targeting circRNAs may be a promising approach for the treatment of AMI. In our previous study, we established a hypoxia model on H9c2 cardiomyocytes to simulate AMI in vitro, and tested the expression of several circRNAs associated with organ injury. The results suggested that hypoxia treatment increased the level of *circANKIB1* in H9c2 cells. The *circANKIB1* has been reported to promote Schwann cell proliferation,

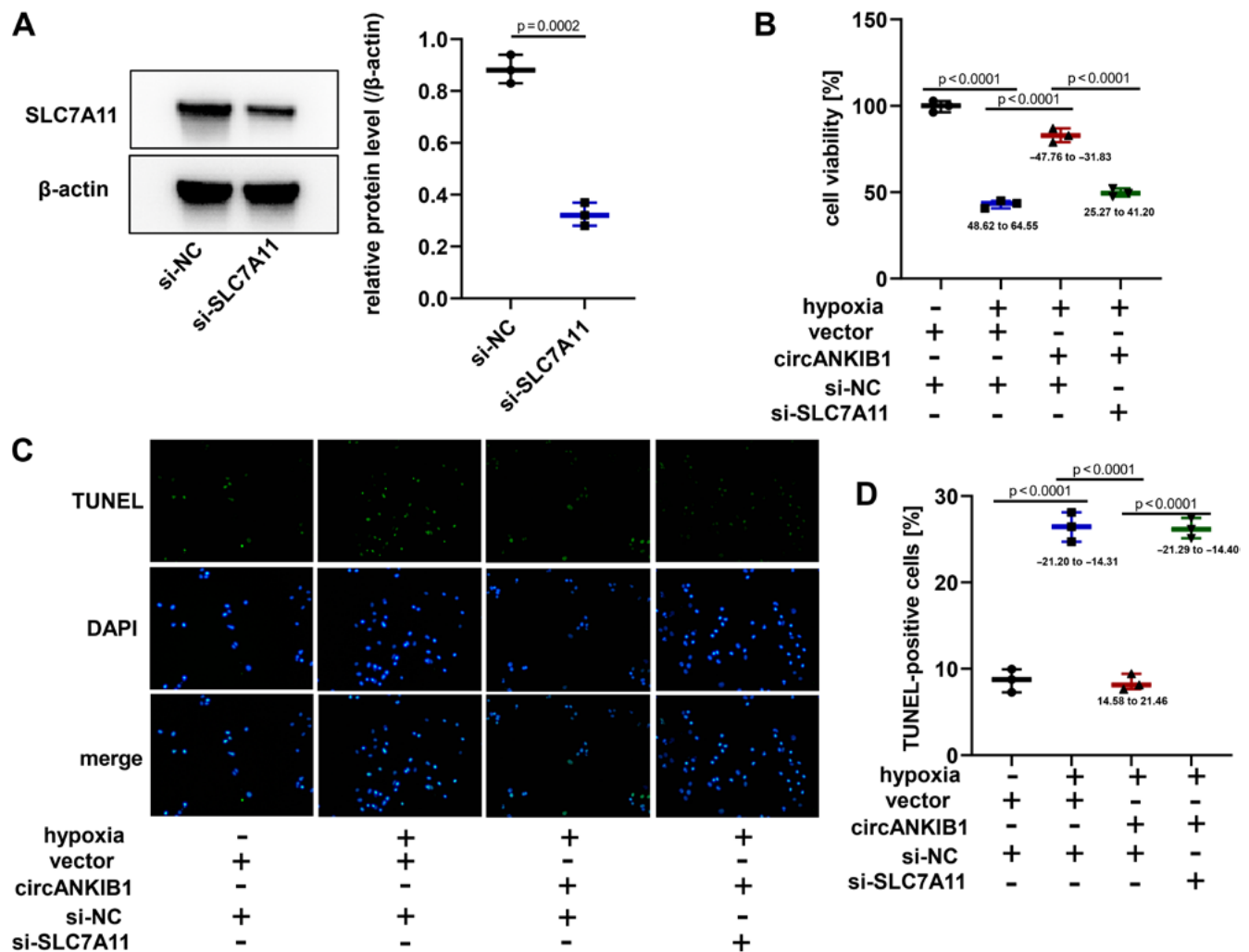


Fig. 6. *SLC7A11* silencing reversed the decreased apoptotic effects of *circANKIB1* overexpression on hypoxia-induced cardiomyocyte injury. **A.** The decreased protein level of *SLC7A11* was estimated via western blotting analysis ($p = 0.001$, $n = 3$, Student's *t*-test); **B.** Methyl thiazolyl tetrazolium (MTT) assay revealed that cell viability restored through *circANKIB1* overexpression was significantly reduced by *SLC7A11* silencing ($p = 0.001$, $n = 3$, analysis of variance (ANOVA) test); **C,D.** Terminal deoxynucleotidyl transferase dUTP nick end labeling (TUNEL) assay indicated that cell apoptosis was markedly increased when compared with *circANKIB1* overexpression transfection in hypoxia-induced H9c2 cells ($p = 0.001$, $n = 3$, ANOVA test)

thereby exerting a protective role in peripheral nerve injury.¹⁵ However, whether *circANKIB1* affects hypoxia-induced cardiomyocytes remains unclear. This work demonstrated that *circANKIB1* was mainly localized in the cytoplasm of H9c2 cardiomyocytes and that the overexpression of *circANKIB1* effectively restored the viability of H9c2 cardiomyocytes that was reduced by hypoxia exposure.

Ferroptosis is a new cell death pattern, different from apoptosis, autophagy and pyrodeath, which is induced by iron-dependent MDA,³⁷ during which iron levels are notably elevated. An overload of ferrous ions causes ROS accumulation, which triggers the production of lipid peroxides such as MDA.³⁸ Furthermore, GPX4 acts as an effective terminator of ferroptosis, capable of converting toxic lipids into non-toxic lipids.³³ Accumulating evidence highlights that ferroptosis is tightly correlated to the occurrence of CVDs, including AMI.³⁷ Interestingly, the present study revealed that the overexpression of *circANKIB1* decreased the level of iron, ROS and MDA, but increased GPX4 expression in hypoxia-induced H9c2

cells. All these data indicated that *circANKIB1* suppressed ferroptosis in our in vitro model.

The circRNAs are regarded as the sponge of miRNAs, regulating their functional role.³⁹ Bioinformatics analysis illustrated that *miR-452-5p* was a potential miRNA target of *circANKIB1*, which was confirmed with luciferase activity that validated the interaction between *circANKIB1* and *miR-452-5p*. The *miR-452-5p* is a vital miRNA that participates in various intracellular activities, including tumorigenesis⁴⁰ and chronic contractile injury.⁴¹ The present study demonstrated a significant upregulation of *miR-452-5p* in H9c2 cardiomyocytes after hypoxia exposure. The overexpression of *miR-452-5p* effectively eliminated the effect of *circANKIB1* on hypoxia-induced H9c2 cell injury and ferroptosis, indicating that *circANKIB1* protected cardiomyocytes from hypoxia by sponging *miR-452-5p*.

Recent studies have confirmed that miRNAs can block the expression of target genes by binding to the 3'UTR of mRNAs.⁴² This study showed that *SLC7A11* was a direct

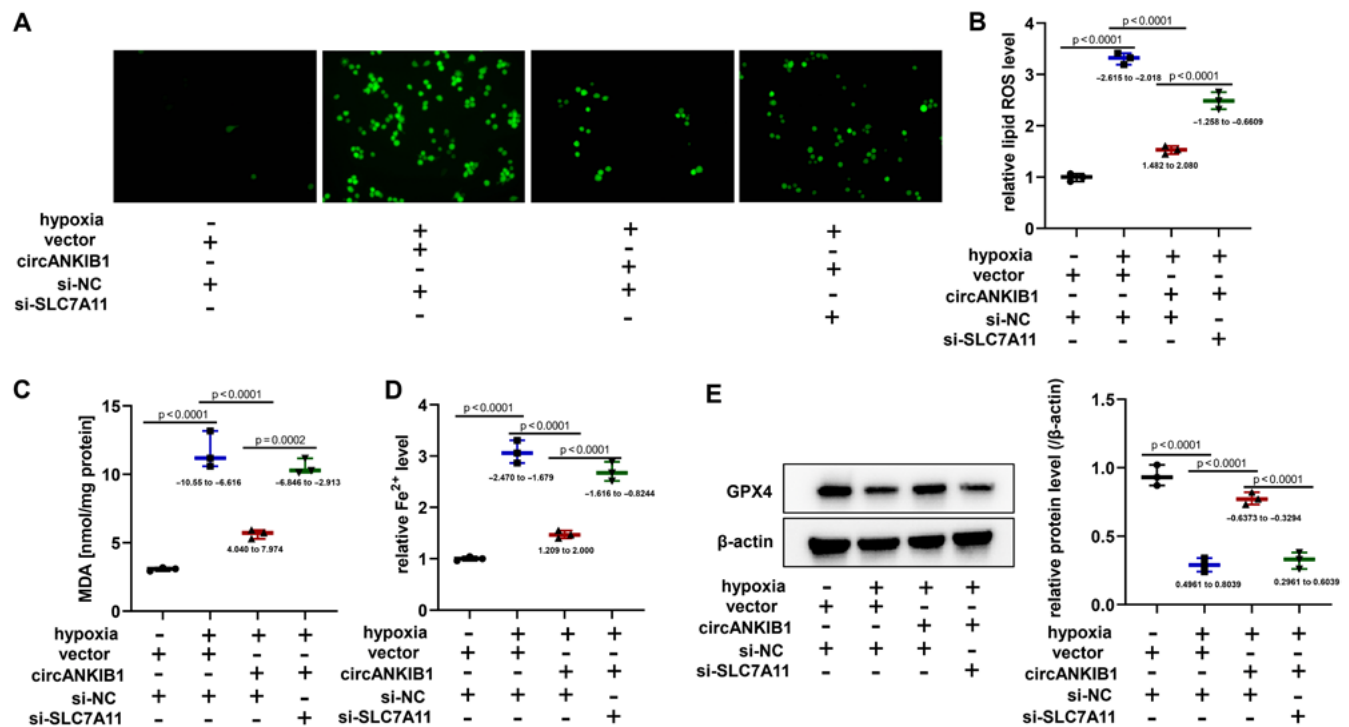


Fig. 7. Downregulation of *SLC7A11* reversed the decreased ferroptosis effect of *circANKIB1* overexpression on hypoxia-induced H9c2 cardiomyocytes. A–D. The levels of reactive oxygen species (ROS) (A,B), malondialdehyde (MDA) (C) and ferrous ion (Fe^{2+}) (D) were markedly decreased after transfection with si-*SLC7A11* when tested using corresponding kits ($p = 0.001$, $n = 3$, analysis of variance (ANOVA) test); E. GPX4 expression increased by *circANKIB1* overexpression and was effectively counteracted by *SLC7A11* knockdown, as analyzed using western blotting analysis ($p = 0.001$, $n = 3$, ANOVA test)

target of *miR-452-5p*. The *SLC7A11* has previously been reported to inhibit oxidative stress and maintain GSH levels, thereby eliminating the occurrence of ferroptosis.⁴³ Emerging evidence showed that *SLC7A11* plays a positive role in protecting cardiomyocytes.⁴³ Our study showed that hypoxia significantly reduced *SLC7A11* expression in cardiomyocytes, which was notably counteracted by *miR-452-5p* inhibitors or *circANKIB1* overexpression. Additionally, the *SLC7A11* knockdown effectively eliminated the protective effect of *circANKIB1* overexpression on cardiomyocyte injury and hypoxia-induced ferroptosis.

Limitations

There are some limitations to this study. First, there no animal experiments were conducted under the AMI model to verify whether *circANKIB1* exerts cardioprotective effects in vivo. In addition, human and mouse cardiomyocytes need to be introduced to further validate these findings. In terms of data analysis, the Shapiro–Wilk test and Levene’s test have very low power at such a small sample size. In future studies, we will increase the sample size to ensure that the results of the statistical analysis are more accurate.

Conclusions

In conclusion, this study revealed that *circANKIB1* alleviates hypoxia-induced cardiomyocyte injury and ferroptosis

by modulating *miR-452-5p/SLC7A11* signaling, providing a potential therapeutic target for patients with AMI.

ORCID iDs

Gang Li <https://orcid.org/0009-0007-4604-2184>

Xiaolei Tang <https://orcid.org/0000-0002-3751-1643>

Huaping Tang <https://orcid.org/0009-0006-1191-3560>

References

- Benjamin EJ, Virani SS, Callaway CW, et al. Heart Disease and Stroke Statistics – 2018 update: A report from the American Heart Association. *Circulation*. 2018;137(12):e67–e492. doi:10.1161/CIR.0000000000000558
- Anderson JL, Morrow DA. Acute myocardial infarction. *N Engl J Med*. 2017;376(21):2053–2064. doi:10.1056/NEJMr1606915
- Tang Q, Li MY, Su YF, et al. Absence of *miR-223-3p* ameliorates hypoxia-induced injury through repressing cardiomyocyte apoptosis and oxidative stress by targeting *KLF15*. *Eur J Pharmacol*. 2018;841:67–74. doi:10.1016/j.ejphar.2018.10.014
- Huang L, Guo B, Liu S, Miao C, Li Y. Inhibition of the lncRNA *Gpr19* attenuates ischemia–reperfusion injury after acute myocardial infarction by inhibiting apoptosis and oxidative stress via the *miR-324-5p/Mtfr1* axis. *IUBMB Life*. 2020;72(3):373–383. doi:10.1002/iub.2187
- Ebbesen KK, Kjems J, Hansen TB. Circular RNAs: Identification, biogenesis and function. *Biochim Biophys Acta*. 2016;1859(1):163–168. doi:10.1016/j.bbagr.2015.07.007
- Li X, Yang L, Chen LL. The biogenesis, functions, and challenges of circular RNAs. *Mol Cell*. 2018;71(3):428–442. doi:10.1016/j.molcel.2018.06.034
- Patop IL, Wüst S, Kadener S. Past, present, and future of circRNAs. *EMBO J*. 2019;38(16):e100836. doi:10.15252/embj.2018100836
- Gao JL, Chen G, He HQ, Wang J. CircRNA as a new field in human disease research [in Chinese]. *Zhongguo Zhong Yao Za Zhi*. 2018;43(3):457–462. doi:10.19540/j.cnki.cjcmm.20171106.012
- Altesha M, Ni T, Khan A, Liu K, Zheng X. Circular RNA in cardiovascular disease. *J Cell Physiol*. 2019;234(5):5588–5600. doi:10.1002/jcp.27384

10. Wang Y, Liu B. Circular RNA in diseased heart. *Cells*. 2020;9(5):1240. doi:10.3390/cells9051240
11. Ren K, Li B, Jiang L, et al. Circ_0023461 silencing protects cardiomyocytes from hypoxia-induced dysfunction through targeting Mir-370-3p/Pde4d signaling. *Oxid Med Cell Longev*. 2021;2021:8379962. doi:10.1155/2021/8379962
12. Wang S, Cheng Z, Chen X, Lu G, Zhu X, Xu G. CircUBXN7 mitigates H/R-induced cell apoptosis and inflammatory response through the miR-622-MCL1 axis. *Am J Transl Res*. 2021;13(8):8711–8727. PMID:34539989.
13. Tang J, Duan G, Wang Y, Wang B, Li W, Zhu Z. Circular RNA_ANKIB1 accelerates chemo-resistance of osteosarcoma via binding microRNA-26b-5p and modulating enhancer of zeste homolog 2. *Bioengineered*. 2022;13(3):7351–7366. doi:10.1080/21655979.2022.2037869
14. Du YX, Guo LX, Pan HS, Liang YM, Li X. Circ_ANKIB1 stabilizes the regulation of miR-19b on SOCS3/STAT3 pathway to promote osteosarcoma cell growth and invasion. *Hum Cell*. 2020;33(1):252–260. doi:10.1007/s13577-019-00298-6
15. Mao S, Zhang S, Zhou S, et al. A Schwann cell-enriched circular RNA circ-Ankib1 regulates Schwann cell proliferation following peripheral nerve injury. *FASEB J*. 2019;33(11):12409–12424. doi:10.1096/fj.201900965R
16. Mirahmadi Y, Nabavi R, Taheri F, et al. MicroRNAs as biomarkers for early diagnosis, prognosis, and therapeutic targeting of ovarian cancer. *J Oncol*. 2021;2021:3408937. doi:10.1155/2021/3408937
17. Ma X, Liu C, Gao C, et al. circRNA-associated ceRNA network construction reveals the circRNAs involved in the progression and prognosis of breast cancer. *J Cell Physiol*. 2020;235(4):3973–3983. doi:10.1002/jcp.29291
18. Kobayashi M, Suhara T, Baba Y, Kawasaki NK, Higa JK, Matsui T. Pathological roles of iron in cardiovascular disease. *Curr Drug Targets*. 2018;19(9):1068–1076. doi:10.2174/1389450119666180605112235
19. Fang X, Wang H, Han D, et al. Ferroptosis as a target for protection against cardiomyopathy. *Proc Natl Acad Sci U S A*. 2019;116(7):2672–2680. doi:10.1073/pnas.1821022116
20. Stockwell BR, Friedmann Angeli JP, Bayir H, et al. Ferroptosis: A regulated cell death nexus linking metabolism, redox biology, and disease. *Cell*. 2017;171(2):273–285. doi:10.1016/j.cell.2017.09.021
21. Zheng J, Conrad M. The metabolic underpinnings of ferroptosis. *Cell Metab*. 2020;32(6):920–937. doi:10.1016/j.cmet.2020.10.011
22. Koppula P, Zhuang L, Gan B. Cystine transporter SLC7A11/xCT in cancer: Ferroptosis, nutrient dependency, and cancer therapy. *Protein Cell*. 2021;12(8):599–620. doi:10.1007/s13238-020-00789-5
23. Zhou Y, Li X, Zhao D, Li X, Dai J. Long non-coding RNA MEG3 knock-down alleviates hypoxia-induced injury in rat cardiomyocytes via the miR-325-3p/TRPV4 axis. *Mol Med Rep*. 2021;23(1):18. doi:10.3892/mmr.2020.11656
24. Tan J, Pan W, Chen H, et al. Circ_0124644 serves as a ceRNA for Mir-590-3p to promote hypoxia-induced cardiomyocytes injury via regulating Sox4. *Front Genet*. 2021;12:667724. doi:10.3389/fgene.2021.667724
25. Bustin SA, Benes V, Garson JA, et al. The MIQE guidelines: Minimum information for publication of quantitative real-time PCR experiments. *Clin Chem*. 2009;55(4):611–622. doi:10.1373/clinchem.2008.112797
26. Liu B, Guo K. CircRbms1 knockdown alleviates hypoxia-induced cardiomyocyte injury via regulating the miR-742-3p/FOXO1 axis. *Cell Mol Biol Lett*. 2022;27(1):31. doi:10.1186/s11658-022-00330-y
27. Zhang Y, Li Z, Wang J, Chen H, He R, Wu H. CircTRRAP knockdown has cardioprotective function in cardiomyocytes via the signal regulation of mir-370-3p/PAWR axis. *Cardiovasc Ther*. 2022;2022:7125602. doi:10.1155/2022/7125602
28. Lan Z, Wang T, Zhang L, Jiang Z, Zou X. CircSLC8A1 exacerbates hypoxia-induced myocardial injury via interacting with Mir-214-5p to upregulate TEAD1 expression. *Int Heart J*. 2022;63(3):591–601. doi:10.1536/ihj.21-547
29. Dai R, Yang X, He W, Su Q, Deng X, Li J. LncRNA AC005332.7 Inhibited ferroptosis to alleviate acute myocardial infarction through regulating mir-331-3p/CCND2 axis. *Korean Circ J*. 2023;53(3):151–167. doi:10.4070/kcj.2022.0242
30. Zhang Z, Yang W, Ma F, et al. Enhancing the chemotherapy effect of Apatinib on gastric cancer by co-treating with salidroside to reprogram the tumor hypoxia micro-environment and induce cell apoptosis. *Drug Deliv*. 2020;27(1):691–702. doi:10.1080/10717544.2020.1754528
31. Kietzmann T, Samoylenko A, Roth U, Jungermann K. Hypoxia-inducible factor-1 and hypoxia response elements mediate the induction of plasminogen activator inhibitor-1 gene expression by insulin in primary rat hepatocytes. *Blood*. 2003;101(3):907–914. doi:10.1182/blood-2002-06-1693
32. Ma S, Sun L, Wu W, Wu J, Sun Z, Ren J. USP22 protects against myocardial ischemia-reperfusion injury via the SIRT1-p53/SLC7A11-dependent inhibition of ferroptosis-induced cardiomyocyte death. *Front Physiol*. 2020;11:551318. doi:10.3389/fphys.2020.551318
33. Yang WS, SriRamaratnam R, Welsch ME, et al. Regulation of ferroptotic cancer cell death by GPX4. *Cell*. 2014;156(1–2):317–331. doi:10.1016/j.cell.2013.12.010
34. Gong X, Wu G, Zeng C. Role of circular RNAs in cardiovascular diseases. *Exp Biol Med (Maywood)*. 2019;244(2):73–82. doi:10.1177/1535370218822988
35. Lin F, Zhao G, Chen Z, et al. circRNA-miRNA association for coronary heart disease. *Mol Med Report*. 2019;19(4):2527–2536. doi:10.3892/mmr.2019.9905
36. Jin L, Zhang Y, Jiang Y, Tan M, Liu C. Circular RNA Rbms1 inhibited the development of myocardial ischemia-reperfusion injury by regulating miR-92a/BCL2L1 signaling pathway. *Bioengineered*. 2022;13(2):3082–3092. doi:10.1080/21655979.2022.2025696
37. Li M, Wang ZW, Fang LJ, Cheng SQ, Wang X, Liu NF. Programmed cell death in atherosclerosis and vascular calcification. *Cell Death Dis*. 2022;13(5):467. doi:10.1038/s41419-022-04923-5
38. Wang M, Liu CY, Wang T, et al. (+)-Clausenamide protects against drug-induced liver injury by inhibiting hepatocyte ferroptosis. *Cell Death Dis*. 2020;11(9):781. doi:10.1038/s41419-020-02961-5
39. Kulcheski FR, Christoff AP, Margis R. Circular RNAs are miRNA sponges and can be used as a new class of biomarker. *J Biotechnol*. 2016;238:42–51. doi:10.1016/j.jbiotec.2016.09.011
40. Lin X, Han L, Gu C, et al. MiR-452-5p promotes colorectal cancer progression by regulating an ERK/MAPK positive feedback loop. *Aging (Albany NY)*. 2021;13(5):7608–7626. doi:10.18632/aging.202657
41. Tian Y, Sun L, Qi T. Long noncoding RNA GAS5 ameliorates chronic constriction injury induced neuropathic pain in rats by modulation of the miR-452-5p/CEL2F2 axis. *Can J Physiol Pharmacol*. 2020;98(12):870–877. doi:10.1139/cjpp-2020-0036
42. Fabian MR, Sonenberg N, Filipowicz W. Regulation of mRNA translation and stability by microRNAs. *Annu Rev Biochem*. 2010;79:351–379. doi:10.1146/annurev-biochem-060308-103103
43. Li Y, Yan J, Zhao Q, Zhang Y, Zhang Y. ATF3 promotes ferroptosis in sorafenib-induced cardiotoxicity by suppressing Slc7a11 expression. *Front Pharmacol*. 2022;13:904314. doi:10.3389/fphar.2022.90431